



Latest updates: <https://dl.acm.org/doi/10.1145/3447993.3448631>

RESEARCH-ARTICLE

One tag, two codes: identifying optical barcodes with NFC

ZHENLIN AN, The Hong Kong Polytechnic University, Hong Kong, Hong Kong, Hong Kong

QIONGZHENG LIN, The Hong Kong Polytechnic University, Hong Kong, Hong Kong, Hong Kong

XIAOPENG ZHAO, The Hong Kong Polytechnic University, Hong Kong, Hong Kong, Hong Kong

LEI YANG, The Hong Kong Polytechnic University, Hong Kong, Hong Kong, Hong Kong

DONGLIANG ZHENG, Donghua University, Shanghai, Shanghai, China

GUIQING WU, Donghua University, Shanghai, Shanghai, China

[View all](#)

Open Access Support provided by:

The Hong Kong Polytechnic University

Donghua University



PDF Download
3447993.3448631.pdf
27 January 2026
Total Citations: 4
Total Downloads: 644

Published: 09 September 2021

[Citation in BibTeX format](#)

ACM MobiCom '21: The 27th Annual International Conference on Mobile Computing and Networking
October 25 - 29, 2021
Louisiana, New Orleans

Conference Sponsors:
SIGMOBILE

One Tag, Two Codes: Identifying Optical Barcodes with NFC

Zhenlin An[†], Qiongzheng Lin[†], Xiaopeng Zhao[†], Lei Yang[†]
Dongliang Zheng[‡], Guiqing Wu[‡], Shan Chang[§]

[†]Department of Computing, The Hong Kong Polytechnic University

[‡]College of Materials Science and Engineering, Donghua University

[§]School of Computer Science and Technology, Donghua University

ABSTRACT

Barcodes and NFC have become the de facto standards in the field of automatic identification and data capture. These standards have been widely adopted for many applications, such as mobile payments, advertisements, social sharing, admission control, and so on. Recently, considerable demands require the integration of these two codes (barcode and NFC code) into a single tag for the functional complementation. To achieve the goal of “one tag, two codes” (OTTC), this work proposes CoilCode, which takes advantage of the printed electronics to fuse an NFC coil antenna into a QR code on a single layer. The proposed code could be identified by cameras and NFC readers. With the use of the conductive inks, QR code and NFC code have become an essential part of each other: the modules of the QR code facilitate the NFC chip in harvesting energy from the magnetic field, while the NFC antenna itself represents bits of the QR code. Compared to the prior dual-layer OTTC, CoilCode is more compact, cost-effective, flimsy, flexible, and environment-friendly, and also reduces the fabrication complexity considerably. We prototyped hundreds of CoilCodes and conducted comprehensive evaluations (across 4 models of NFC chips and 8 kinds of NFC readers under 13 different system configurations). CoilCode demonstrates high-quality identification results for QR code and NFC functions on a wide range of inputs and under different distortion effects.

CCS CONCEPTS

- Networks → Mobile networks.

KEYWORDS

Cross-Technology Communication; NFC; Barcodes; Reinforcement Learning

ACM Reference Format:

Zhenlin An[†], Qiongzheng Lin[†], Xiaopeng Zhao[†], Lei Yang[†], Dongliang Zheng[‡], Guiqing Wu[‡], Shan Chang[§]. 2021. One Tag, Two Codes: Identifying Optical Barcodes with NFC. In *The 27th Annual International Conference On Mobile Computing And Networking (ACM MobiCom '21)*, October 25–29,

Permission to make digital or hard copies of all or part of this work for personal or classroom use is granted without fee provided that copies are not made or distributed for profit or commercial advantage and that copies bear this notice and the full citation on the first page. Copyrights for components of this work owned by others than ACM must be honored. Abstracting with credit is permitted. To copy otherwise, or republish, to post on servers or to redistribute to lists, requires prior specific permission and/or a fee. Request permissions from permissions@acm.org.

ACM MobiCom '21, October 25–29, 2021, New Orleans, LA, USA

© 2021 Association for Computing Machinery.

ACM ISBN 978-1-4503-8342-4/21/10...\$15.00

<https://doi.org/10.1145/3447993.3448631>

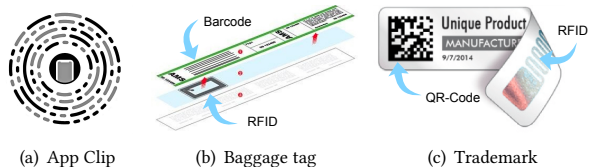


Fig. 1: One tag two codes. These dual-layer tags (on which a barcode and an RFID are attached in two separate layers) were invented to meet the business demand of requiring simultaneously.

2021, New Orleans, LA, USA. ACM, New York, NY, USA, 13 pages. <https://doi.org/10.1145/3447993.3448631>

1 INTRODUCTION

Automatic identification and data capture (AIDC) refers to the technologies of automatically identifying objects and collecting data about them without human involvement. Nowadays, the barcodes (like QR-Code) and radio frequency identification (RFID, such as NFC) have become the most widely adopted AIDC methods. They facilitate the mobile phone usage of billions of people throughout the world and offer diverse services, ranging from advertisement to mobile payment. For example, a QR code or an NFC code (aka NFC tag) allows users to conveniently pay or transfer money by scanning the codes with their mobile phones.

As pioneers of short-range and contactless communication technology, barcode and RFID almost function similarly in many scenarios, e.g., mobile payment, business promotion, social sharing, admission control, membership, and so on, both of which are used to store short data for AIDC. Barcodes (representing data in black/white bars or dot matrix) are read through optical reflections, while RFID tags (using microchips to store data) are identified through RF signals. Such different underlying rationales lead to their difference in the technical features. Barcodes scanners must keep a line-of-sight with each code. In contrast, RFID tags are scanned once they are proximate to the “near-field” of the reader or even blocked from non-metal obstacles. Barcodes are much more widely adopted than RFID on the consumer market because cameras have already become a standard configuration of a smart phone.

Despite similar functionality, the RFID and barcode cannot take the place of the other in particular circumstances. This would cause practical difficulty in choosing the proper AIDC systems. Particularly, a large number of business scenarios require the joint use of barcode and RFID. Both codes are combined into a single tag, known as “one tag, two codes” (OTTC). In the early part of this year, Apple Corp. introduced a new type of OTTC, called “App Clip”, which actually encodes a URL through a private barcode and

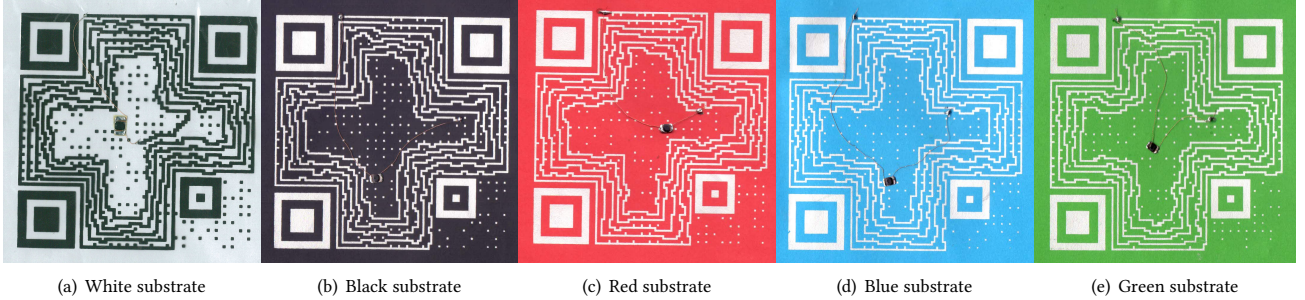


Fig. 2: Scanning copies of our CoilCodes. These codes are printed on standard A4 papers in the size of $7 \times 7 \text{ cm}^2$. The CoilCode shown in (a) is made of black carbon nanotubes on a white paper. The CoilCodes shown in (b)~(e) are made of white nanosilver particles on colorful A4 papers. The thickness of the codes is around $20 \mu\text{m}$. The small black components above the papers are the NFC chips, which are connected to coil antennas with flywires.

implants an NFC chip inside [1]. Fig. 1(a) shows an example of the App clip, which can be read by being tapped on or scanned by the camera. The App clip targets at enhancing the user experience when doing the payment, registration, messaging, etc. Similarly, large-scaled airports integrated with automatic sorting systems use RFID based baggage tags for the sortation [36]. However, the destination airports where the baggage is delivered to, are still using barcode recognition systems only. Fig. 1(b) shows a typical OTTC for baggage. Such similar open transportation systems must use OTTC for cross-domain compatibility. Fig. 1(c) shows the use of OTTC in warehouses or supermarkets for asset management, which needs to scan continuously and quickly a batch of assets via RFID to determine if something is missing or out of order. These tags also allow customers to scan the information of a single item through the barcode.

The conventional OTTC simply attaches an RFID code and a barcode on two separate layers. This naive solution can reduce the occupying area of the tag (which is quite important in practice) and avoid mutual interference, i.e., the barcode might be blocked by the RFID antenna. However, the procedure of fabricating such a dual-layer OTTC is rather complicated. It mainly requires two main steps. The first step is to insert the copper antenna and NFC chips into the hidden layer of a self-adhesive label, which leaves the top layer blank. After this step, the shape and the size of the tag cannot be changed anymore because the copper coils are not adjustable. In the second step, the blank tag is fed as input into an RFID printer [15], which prints QR code on the blank layer and writes ID to the NFC chip. The interface of the printer must keep aligned with the shape of the input tag. Both tags and printers must be redesigned to fit new demands. Particularly, in the current manufacturing procedure, the two steps are done by two separated manufacturers: NFC providers and printer providers. The downstream users must collaborate with the two different providers to design personalized tags at an enormous cost, making the customized tags nearly impossible.

Is there an alternative approach to buttering the bread on both sides? Recently, printed electronics offer a breakthrough [21, 25, 31]. It allows us to print customized circuits on many flexible materials (such as textiles and paper) by using low-cost conductive inks (e.g., metal nanoparticles, carbon nanotubes, graphene, etc.). For example, the recent work [31] adopts the graphene inks to successfully produce a customized wireless antenna that can operate from MHz to tens of GHz for energy harvesting and wireless communication.

Table 1: Comparison with other techniques

Techs	AppClip	Traditional OTTC	CoilCode
Complexity	Two steps	Two steps	One step
Cost	$\sim 10 \text{ cent}$	$\sim 10 \text{ cent}$	$\sim 1 \text{ cent}$
Bendable	No	No	Yes
Thickness	$\sim 0.5\text{mm}$	$\sim 0.5\text{mm}$	$20 \mu\text{m}$
Convenience	Low	Low	High
Compatibility	50%	100%	100%
Env.-friendly	No	No	Yes

This new progress inspires us to take advantage of the printed electronics to fabricate a real OTTC on *a single layer*. We observe that an RFID like NFC tag consists of a very *tiny* chip but a *relatively larger* coil antenna, which prevents an RFID from being printed together with a barcode in a limited surface area. Hence, the difficulty in the coexistence of an RFID and a barcode on a single layer is how to fuse the designs of an RFID antenna and a barcode.

To this end, we invent a new type of OTTC, called CoilCode, which fuses a coil antenna into a QR code on a single layer. To better understand the CoilCode, we show some prototypes in Fig. 2. These camera-recognizable QR-codes are composed of conductive inks (metal nanoparticles or carbon nanotubes). Cross-shaped coil antennas for NFC chips are implanted into the QR codes. These two codes are fused seamlessly in the same surface area, achieving a real OTTC. The trick of CoilCode is to string the conductive squares of the QR code (called *modules*) in sequence to form the coil antenna, making the QR code and NFC coil roll into one. Specifically, the modules of QR code facilitate NFC chip to harvest energy from the magnetic field through inductive coupling, while the NFC coil itself represents QR code bits.

CoilCode offers many attractive features. Table 1 compares CoilCode with previous dual-layer solutions from different dimensions. First, as aforementioned, it requires a complicated two-step manufacturing process to produce an on-demand OTTC. CoilCode combines the two steps and offers a one-stop service, allowing downstream users to print codes with personalized shapes and sizes. We believe that our solution will significantly promote industrial upgrading in the near future. Second, a traditional copper-made NFC tag costs about 10 cents while a CoilCode made of nano-silver is around 1 cent. CoilCode cuts the cost of each tag by a factor of 10, which is extremely sensitive for applications (like logistics) that need to process millions of items each year. Third, the presence of RFID antennas (made of hard metal materials, such as copper coils) deprives the paper barcode of the characteristics of bendability and flexibility. By virtue of the conductive inks, CoilCode can be also printed on textiles or bendable surfaces. Fourth, the thickness of a coil antenna is around 0.5 mm but that of a CoilCode is about

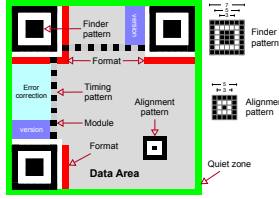


Fig. 3: Structure of a QR code

$20\ \mu\text{m}$. The QR codes printed on an uneven coil surface are vulnerable to be distorted in practice, while CoilCode does not have this issue. Fifth, users are hardly aware of the existence of the RFID in the hidden layer. To address this issue, the App clip or contactless credit payments must show additional signs to remind users of the availability of NFC function. Finally, Superior to Apple clip, CoilCode supports the widely-adopted QR code instead of the Apple private barcodes besides the fuse design. In summary, CoilCodes are compact, flimsy, flexible, cost-effective, environment-friendly (does not require copper), and reduce the fabrication complexity considerably.

The fundamental challenge of CoilCode is from the divergence in the design philosophy of the two codes. The distribution of black modules in a QR code should be scattered to avoid the emergence of a predefined continuous pattern (e.g., finder or timing pattern). On the contrary, the coil antenna of NFC demands connectivity. To address this issue, we explore a minimally-invasive solution, which implants an NFC coil into a QR code. Specifically, we first slice each module of the QR code into nine sections similar to a tic-tac-toe board and convert such a sparse QR code to a grid. Then, the design is boiled down to the problem of finding the longest spiral path (NFC coil) in a grid.

The second challenge is derived from the longest-path searching, which has been proven NP-hard [7]. Worse, the searched path must fully meet four physical constraints (see §3) resulted from the electronic characteristics. To address this issue, we convert the design problem to play a “game”, which is a combination of Maze Game [3, 8] and Snake Game [13]. In the game, an agent starts from a corner and moves towards the center of the grid. It elongates the path whenever traversing an unblock cell, and each movement is ruled by the four constraints. The spiral coil antenna for NFC will be naturally constructed if the agent wins the game, i.e., it successfully finds the optimal sequence of cells in which the accumulated sum of rewards is maximal. To play this game, we resort to deep reinforcement learning, which has shown great power in playing similar games like AlphaGo [33].

Contributions. We totally fabricated 200 prototypes of CoilCode using the commercial off-the-shelf (COTS) conductive inks and NFC chips. These prototypes are evaluated extensively across 4 models of NFC chips and 8 types of NFC readers. We also manually scanned the QR codes using 13 different system configurations, to validate the reliability and the readability of these CoilCodes. In summary, we make the following contributions:

- We present the first printed and single-layer OTTC that can be recognized by barcode scanners and NFC readers using the technology of printed electronics inks.
- We take advantage of deep reinforcement learning to fuse two codes, which reserves all characteristics of a barcode and can be also reused as an NFC coil antenna.

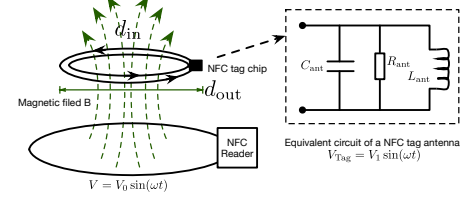


Fig. 4: Schematic illustration of NFC

- Finally, we prototype our design with COTS conductive inks and demonstrate the feasibility of CoilCode with comprehensive evaluations.

2 BACKGROUND

Our design is not limited to any specific type of barcode or RFID. With the QR code and HF NFC as the de facto standards, we choose them to present our design. However, we must state that the design can be extended to any type of barcode or RFID easily. In this section, we first introduce their backgrounds.

2.1 Quick Response Code

Quick Response (QR) code is a two-dimensional barcode consisting of black and white squares where the square is called a *module*. Each module represents one-bit information, i.e., 0 or 1. A QR code contains $(17 + 4V) \times (17 + 4V)$ bits or modules where V is the version number and $V \leq 40$. Fig. 3 shows the typical structure of a QR code [24]. Specifically, the three homocentric-squares on the three corners are called *finder patterns*, each of which consists of 7×7 modules. The finder pattern is used to detect the position of the QR Code in all directions (360°). By arranging this pattern at the three corners, the symbol’s position, size, and angle can be detected. Two *timing patterns* target at correcting the central coordinate of the data modules when the symbol is distorted or when an error exists. They are composed of with-black-white modules arranged alternately. Two timing patterns are arranged in the vertical and horizontal directions respectively. The *alignment pattern* is a small-sized homocentric-square (consisting of 5×5 modules) on the bottom right corner. It helps correct the nonlinear distortion of a QR code. When $V > 6$, multiple alignment patterns are required. Apart from the pattern blocks, the encoded version (blue area) and format (red area) information are placed around the finder patterns. Except for the above, all remaining modules are used for storing the data and error correction code. The QR code utilizes RS codes for providing the error-correcting capability. There are four error correction levels that can recover 7% (L), 15% (M), 25% (Q) and 30% (H) error codewords.

2.2 Near-Field Communication

Ampère’s circuital law states that when a coil is placed in a magnetic field, a current is induced in this coil. This phenomenon is called *inductive coupling*, which is the physical principle of NFC. Specifically, an HF NFC reader creates a low-frequency magnetic field at 13.56 MHz. The magnetic inductive coupling transfers the power from the reader to the NFC tag. NFC antennas act as air core transformers. They communicate with each other by changing the intensity of the magnetic field. Fig. 4 illustrates the schematic

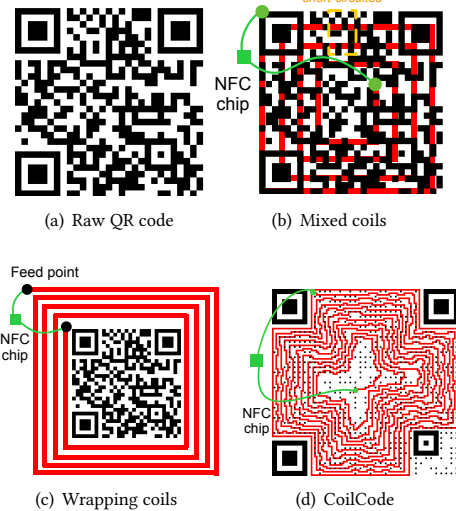


Fig. 5: Comparison of potential OTTC designs. The QR code and coil antenna are both in black. To be distinguishable, the coil antennas are shown in red in the figures.

diagram of an NFC system. The induced voltage in the NFC tag is proportional to the mutual inductance between the coils and the strength of the magnetic field. The antenna of the NFC tag can be designed with different shapes, depending on the application requirements. The main parameter is the equivalent inductance L_{ant} of the antenna, which can be approximated:

$$L_{\text{ant}} = K_1 \times \mu_0 \times n^2 \times \frac{l}{1 + K_2 \cdot p} \quad (1)$$

where K_1 and K_2 are the constants dependent on the antenna layout. μ_0 is a constant equal to $4\pi \cdot 10^{-7}$ H/m. l_{in} and l_{out} are the approximated diameters of the inner and outer coil turns. $l = (l_{\text{out}} + l_{\text{in}})/2$ is the average diameter, $p = (l_{\text{out}} - l_{\text{in}})/(l_{\text{out}} + l_{\text{in}})$, and n is the number of turns. The efficiency of an NFC antenna is in direct proportion to n and l . Concisely, *the performance of inductive coupling is proportional to the length of the coil ($\sim n \times l$)*.

3 DESIGN

The objective of CoilCode is to design a dual-purpose OTTC, which can be recognized by a camera or an NFC reader. The data encoded by the QR code and the data stored in the NFC chip may or may not be consistent and is up to the upper-layer application. The salient feature of printed electronics is the ability to build the electronic circuit directly onto a substrate. For clarity, we assume that the conductive inks are black, the insulative substrate is white, and no other available colors can be printed out. Actually, the silver-nanoparticle based conductive ink is in white. We will discuss this issue later. In this section, we will introduce the design details.

3.1 CoilCode in a Nutshell

The core concepts behind CoilCode can be best understood with examples. Fig. 5(a) shows the raw QR code which can be scanned using barcode cameras. It encodes a URL linked to the Wikipedia on the QR code. When it is printed out, the black modules are made of conductive ink while the white modules are blank spaces full of insulative substrate. We intend to add a coil antenna onto the QR code

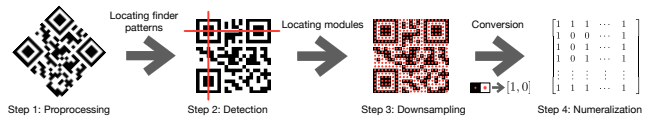


Fig. 6: Recognition of a QR Code. The recognition is a reverse process that converts a QR image back to the bit matrix. The process contains four steps: preprocessing, detection, downsampling, and numeralization.

for the NFC function. Fig. 5(b)-(d) show three possible solutions. Fig. 5(b) shows a simple fusion scheme without increasing floor area, which prints the coil onto the QR code directly. To be distinguishable, the coils are shown in red but are actually in black in the final printed code. This scheme causes mutual interference: the coil ruins the structure of the raw QR code, resulting in the recognition failure; the coil antenna is short-circuited by the black modules of QR code, thereby disabling the inductive coupling. Fig. 5(c) shows a naive but working solution, which prints many turns of coils to wrap the QR code. However, this solution is cumbersome and cost-ineffective because it takes up relatively larger space and consumes more conductive inks, which might be unacceptable in many scenarios where the surface area is quite limited. Fig. 5(d) shows our design which embeds a cross-shaped coil antenna into the QR code. The two ends of the coil are connected to a tiny NFC chip through fly-wires. Our design neither ruins the QR structure nor changes the size of the QR code.

It is easy to calculate how our design outperforms the naive design shown in Fig. 5(c). In terms of size and consumed conductive inks. Suppose the QR code with version V is $L \times L$ in size, then each module is $(L/(17+4V))^2$ in size and thereby the width of the coil antenna equals $L/(17+4V)$. The naive design approximately takes up $(2n/(17+4V)+1)^2 \times$ more area and uses $(2n/(17+4V)+1)^2 \times$ more conductive ink than our design where n is the number of turns. For example, if $L = 10$ cm, $V = 4$, and $n = 10$, the naive design takes up or wastes $2.57 \times$ more space or more conductive inks than ours. Notably, CoilCode provides a better design.

3.2 Sparse QR Code

A QR code is displayed as an image where each bit corresponds to a white or black modules (i.e., small squares). The recognition of a QR code is the reverse process that transforms the scanned image back to the bit matrix by using image processing techniques. Fig. 6 sketches the recognition procedure. In the first step, the image is preprocessed by using binarization, i.e., each pixel is converted to either a black or a white pixel. In the second step, the QR code is detected and located once the three finder patterns are detected. The coordinate system is set up and the whole image is further divided into $(17+4V) \times (17+4V)$ segments, each of which corresponds to a module. Suppose a segment is composed of $M \times M$ pixels, we say that each module is sampled by M^2 times. The *downsampling step* is to re-select the center pixel of each module as the new sample, which is equivalent to reducing the sampling rate from M^2 times to 1 time. Finally, the color of the selected center pixel is used to determine the corresponding bit value: black \rightarrow bit one; white \rightarrow bit zero.

The downsampling step suggests that the recognition client only uses the center pixel of each module for numeralization, which inspired us to generate a sparse QR code. Specifically, we further

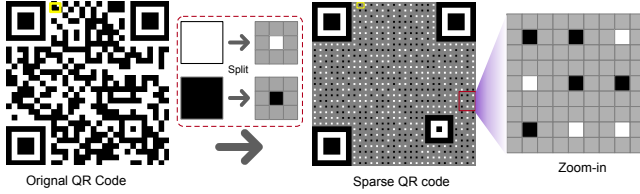


Fig. 7: Illustration of generating a sparse QR code. Each module on the raw QR code is split to 9 submodules like a tic-tac-toe board, where the center submodule has the same color as the original module (white or black) but the other 8 outside submodules are colored with gray. The zoom-in figure shows 81 submodules can be split from 9 modules.

split each module into 3×3 submodules like a tic-tac-toe board. The center submodule is kept the same color as the original module, but the other outside eight submodules are colored with gray. Fig. 7 shows a toy example. Because of downsampling, the outside submodules are irrelevant to the recognition result even if they are filled with other colors. However, the modules constituting the finder and alignment patterns are not split, because the detection of patterns is performed before the downsampling step. It can be also simply viewed that patterns are split but the resulting submodules are maintained as the same color as the raw module.

Consequently, the physical size (the number of pixels) of a sparse QR code remains unchanged, but its logical size (the number of submodules) is enlarged by nine times. A sparse QR code contains $9 \times (17 + 4V) \times (17 + 4V)$ submodules in total. The extra outside submodules provide more available space to accommodate the NFC coil antenna. In the following, we will use the sparse QR code for the design.

3.3 Problem Statement

We consider a sparse QR code as a grid where each submodule is viewed as a cell of the grid. The grid contains three kinds of cells: black, white, and gray cells. The black cells are blocked (i.e., insulative), while the white cells are unblocked (i.e., conductive). The gray cells can be blocked or unblocked in such a rule: a gray cell is changed to an unblocked cell if it is chosen as a part of the NFC antenna; otherwise, it is changed to a blocked cell. In this way, designing an NFC antenna can be formulated as a problem of searching a path in the grid. This path begins from the cell at the top-left corner and goes toward the center cell. The searched path forms a spiral coil antenna. Most importantly, the path-formed spiral antenna should contain sufficient turns to maximize the performance of inductive coupling (see Eqn. 1).

At first glance, it appears that we are searching for the longest path in the grid, which is NP-hard [7]. The problem actually is more difficult than the longest-path problem because the searching algorithm is also constrained by the following optical and electronic conditions:

C1: Structure-invariance. The presence of the spiral coil must not destroy the QR code structure (especially the function patterns), which is the key in the QR code recognition.

C2: Insolutivity. The path must not contain loops on which any two cells can reach each other with multiple routings. A loop will short-circuit the spiral coil. Fig. 8(a) shows a toy example, where the red solid line indicates the searched path. This path does not fulfill the insulative constraint, because the black cell at (3, 2) short-circuits the searched path, making the real path become $(1, 1) \rightarrow$

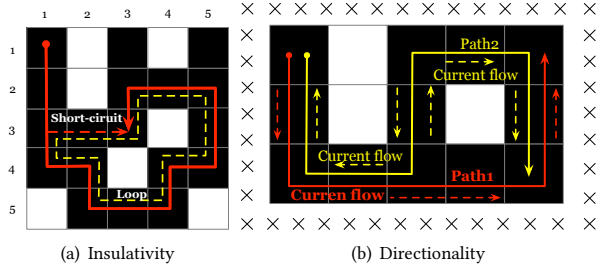


Fig. 8: Illustration of design constraints. (a) The searched path highlighted in red is short-circuited. (b) Path2 contains a Z-turn which causes two inductive currents to flow to two directions.

$(2, 1) \rightarrow (3, 1) \rightarrow (3, 2) \rightarrow (3, 3)$. The short-circuit happens not only at the two horizontally or vertically adjacent cells but also at the two cells that share a corner, e.g., (4, 1) and (3, 2) in the figure. Thus, a specific cell might be short-circuited by any of its eight neighbors.

C3: Directionality. The turning directions of the coil (clockwise or anti-clockwise) must always remain consistent; otherwise, the inductive currents in the two opposite directions will cancel each other. Fig. 8(b) shows the scenario. Suppose magnetic field B is inward to the plane of the paper. The coil along Path2 first turns anti-clockwise and then turns clockwise. As a result, the current induced along the two turns flows to two opposite directions, making the final current zero. In contrast, the direction of Path1 remains consistent although its total length is 2 cells less than the Path2. Thus, a switchback with Z-shaped turns might be the longest but does not meet the directionality constraint.

C4: Tolerance. Some cells can be inverted (e.g., black cells \rightarrow white cells, or vice versa) as needed. However, the total number of inverted cells must be less than the error percent that the correction level tolerates (see §2). For example, the black cell at (3, 2) in Fig. 8(a) and black cell at (2, 3) in Fig. 8(b) should be inverted to avoid short-circuits.

3.4 NFC Antenna Design with RL

We propose a feedback control loop where *context* can be calculated whenever a cell is chosen to join in the path to meet the rigorous constraints mentioned above. A learned *policy* which cells should be selected in the next move; a *reward* is given when a decision is taken, and it helps fine-tune the policy accordingly. This loop falls naturally into the realm of reinforcement learning (RL) [19], which shows great progress in mastering games, such as AlphaGo [33], Atari [33], MOBA Game [34], and so on. Our problem can be viewed as a similar game, which is a combination of the classic Maze Game [3, 8] and Snake Game [13]. In Maze Game, an agent is required to find the shortest path in a grid comprised of the blocked and unblocked cells from a start cell to eat cheese (i.e., destination). In Snake Game, a moving agent elongates its body after successfully eating an apple and dies if it bumps into the edge of the screen or accidentally eats itself (i.e., short-circuited). In our problem domain, the agent starts from a corner and moves towards the center similar to the Maze Game. Meanwhile, similar to the Snake Game, the agent elongates its path whenever it visits an unblocked cell, and fails if it revisited a traversed cell (which causes a short-circuit). The agent experiments and exploits past experiences to find an optimal path. It may fail again and again,

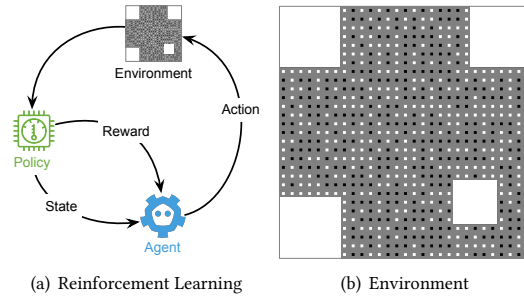


Fig. 9: Illustration of Reinforcement Learning. (a) shows a schematic diagram of RL and (b) shows our environment which is a grid derived from the sparse QR code, where three finder and alignment patterns are marked as unreachable walls.

but after considerable trials and errors (rewards and penalties), it will arrive at the destination. The spiral antenna will be naturally constructed if the agent finds the optimal sequence of states in which the accumulated sum of rewards is the maximal. On account of such similarity, we resort to the deep reinforcement learning (RL), which has shown the great power in “playing” similar games (e.g., AlphaGo) recently.

Reinforcement Learning. An RL system consists of an *environment* and a dynamic *agent* that acts in this environment (e.g., chessboard) in finite discrete lists of time steps [3], as shown in Fig. 9(a). At every time step k , the agent is transiting to a state s_k , and needs to choose an action a_k from a fixed set of possible actions. The decision on which action is taken should depend on the current state only, i.e., the previous action history is irrelevant, which is known as the Markov decision processes (MDP). Specifically, the result of performing action a_k will result in a transition from a current state s_k to a new state $s_{k+1} = T(s_k, a)$, and an immediate reward $r_k = R(s_k, a)$, which is collected by the agent after each action. The reward could be negative, becoming a *penalty*. The $T(\cdot)$ is called *transition function* and $R(\cdot)$ is the *reward function*. The agent’s goal is to collect the maximal total reward during a game. The greedy policy of choosing the action that yields the highest immediate rewards at state s_k may not lead to the maximum total rewards because it may happen to strike all subsequent moves that will yield poor rewards or even penalties. If the agent takes the action sequence of $(a_0, a_1, a_2, \dots, a_K)$, then the resulting total reward \mathcal{R} for this sequence is given by the following:

$$\mathcal{R} = \sum_{k=0}^K R(s_k, a_k) = r_0 + r_1 + \dots + r_K \quad (2)$$

Thus, the goal of RL becomes to find a *policy* function denoted by $\pi(\cdot)$ that maps a state s_k to an optimal action a_k that the agent should take to achieve the maximal total reward \mathcal{R} . The policy $\pi(\cdot)$ indicates which action should be taken at state s_k as below:

$$a_k = \pi(s_k) \quad (3)$$

Once the policy function $\pi(\cdot)$ is built, the agent chooses each action by following it. In the following, we will specify how the RL can be applied in our problem domain.

(1) Environment. Our environment is the grid derived from the sparse QR code. The cells constituting the three finder patterns and the alignment pattern are forcedly colored with white (i.e., blocked) because of the constraint **C1**. Fig. 9(b) shows the environment corresponding to the sparse grid shown in Fig. 7. Initially, the agent

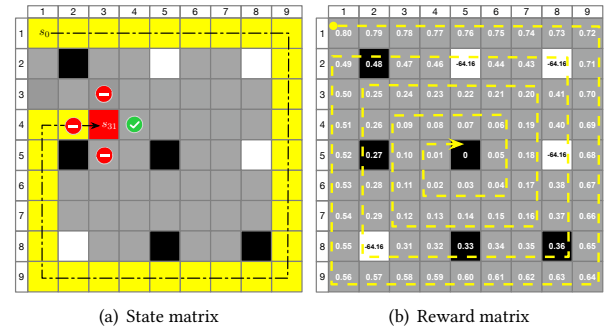


Fig. 10: A Simplified 9 × 9 Environment. (a) shows the state matrix of the 31st step. (b) shows the reward matrix in which each cell is assigned with a reward based on the position of the cell.

is located in the gray cells at the top-left-most corner (start cell) and is heading to a given internal black cell (destination). The destination is a custom-defined parameter. For clarity, we will use another simplified 9 × 9 environments (Fig. 10) to introduce the remaining components in the following.

(2) Actions. Initially, the agent locates at the start cell. It can perform four actions at every step: moving up (\uparrow), moving down (\downarrow), moving left (\leftarrow), and moving right (\rightarrow). Formally, the set of all actions is denoted by \mathcal{A} , i.e., $\mathcal{A} = \{\uparrow, \downarrow, \leftarrow, \rightarrow\}$ and $a_k \in \mathcal{A}$. The action is marked unavailable if it results in the following: (1) the agent moves into walls or beyond boundaries or (2) the agent moves to a visited cell or a cell that causes a short-circuit. Fig. 10(a) shows the simplified 9 × 9 environment where the agent is locating at cell (4, 3) currently. The only available action that the agent can perform is to move right because all other actions will cause short-circuits. Specifically, if the agent moves up, the cell (3, 3) will be connected to cell (1, 2) through cell (2, 2). Similarly, stepping back to cell (4, 2) is also viewed as a short-circuit (cell (4, 3) is short-circuited). If no actions are available in the current step, the game is declared “lose” because it moves to a dead corner. We hope the agent can learn how to “win” the game after considerable training.

(3) State Matrix. At the end of each step, the whole grid is converted into a *state matrix* in which two additional colors (red and yellow) are added. The yellow cells indicate the cells that the agent visited, and the red cell indicates the cell where the agent is currently staying. Fig. 10(a) shows the state matrix of the 31st step (i.e., s_{31}). The grid layout is also contained in the state matrix and thus, our RL algorithm is not limited to a specific QR code. In the following, we will use a deep neural network to fit the policy where the state matrix will be used as the input.

(4) Reward Function. The key of the RL is the reward function, which guides the agent in finding a correct path that meets all aforementioned constraints. The objective in the design of the NFC antenna is twofold: (i) *the path that the agent visited should be in the shape of the spiral coil* and (ii) *the direction that the agent is heading towards should remain consistent* (i.e., clockwise or anti-clockwise). To this end, we create the reward function as follows:

- If the agent moves to a black or a gray cell at (i, j) , the reward is given based on their positions in an $N \times N$ grid:

$$R(i, j) = \begin{cases} 1 - \frac{(M-1)(4(N-M)+2)-2+i+j}{N^2-1} & \text{if } i \leq j \\ 1 - \frac{M(4(N-M)+2)-i-j}{N^2-1} & \text{otherwise} \end{cases} \quad (4)$$

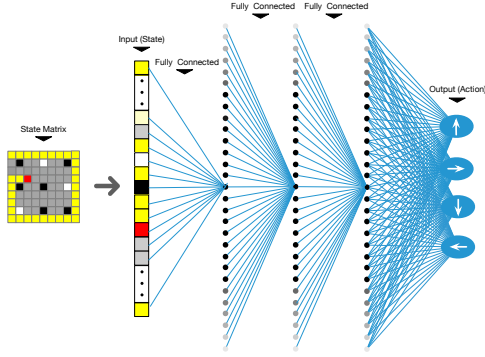


Fig. 11: Schematic illustration of the DQN. The input of the neural network is the state matrix in which different colors are converted to the gray-scale value. The size of three fully-connected hidden layers is identical to the grid size.

where $M = \min(i, j, N - i + 1, N - j + 1)$. Eqn. 4 defines a discrete Archimedean spiral function, in which M indicates the turn index from outside to inside. Fig. 10(b) shows the rewards corresponding to the previous environment (Fig. 10(a)). From the figure, we observe that the reward assigned to a non-white cell is less than one; and the reward decreases spirally from the top-left corner cell to the center cell. Suppose the agent is currently locating at cell $(1, 1)$, it will move to cell $(1, 2)$ instead of $(2, 1)$ because visiting the previous cell gains a higher reward. This way would guide the agent to walk along a spiral path. However, the agent cannot simply pursue a higher reward at each step because the action might be constrained as stated earlier.

- If the agent moves to a white cell, a penalty is given:

$$R(i, j) = -10N_{BG}/3N_W \quad (5)$$

to “discourage” this action, because all cells on the visited path finally will be printed out in black, leading to the color inversion. N_{BG} and N_W are the numbers of black/gray cells and white cells respectively. Once the total reward becomes negative, the agent loses the game (i.e., the antenna design is unacceptable). Placing this rule into perspective, the total percent of white cells that the agent can move to is less than 30% (H-level, C4). Specifically, the reward-related to each gray and black cell is less than one and thus the maximum positive reward is $\mathcal{R}^+ < N_{BG}$. If the percent of visited white cells is greater than 30%, then the penalty (negative reward) $\mathcal{R}^- < 30\% \times N_W \times (-10N_{BG}/3N_W) = -N_{BG}$. Consequently, the total reward $\mathcal{R} = \mathcal{R}^+ + \mathcal{R}^- < N_{BG} - N_{BG} = 0$. Then, the agent loses the game. In Fig. 10(b), because $N = 9$, $N_W = 4$ and $N_{BG} = 77$, the white cells are assigned with a penalty of -64.15 .

- If the agent moves to walls or pattern areas, the reward is negative infinity and the game is immediately lost.

Although all cells are assigned a reward or a penalty, it does not mean the agent will visit all these cells with positive rewards. The agent also needs to consider whether the visit results in “game lose”. If the agent visits the grid based on the yellow routing shown in Fig. 10(b), it will lose the game because of the short-circuit. In short, the reward function only defines the rules rather than presents the answer.

(5) Termination. The game is over for three conditions. First, the agent loses the game if it falls into a dead corner (i.e., no actions are available). Second, the agent loses the game if its total reward

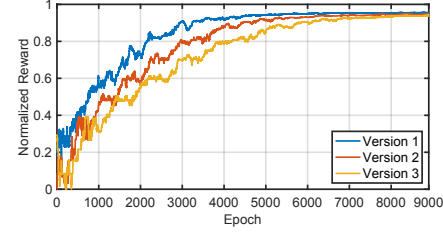


Fig. 12: Training curves tracking the agent’s normalized reward. The training is taken on the QR codes V1, V2, and V3.

becomes negative. Third, the agent wins when it arrives at the destination and achieves $\alpha\mathcal{R}^+$ where \mathcal{R}^+ is the maximal total positive reward. The α is a user-defined parameter (e.g., $\alpha = 60\%$), which is determined by the minimal length of the required NFC antenna in practice. The solution will be achieved if the agent finds the optimal action sequence to accumulate a maximum total reward and solves our problem while doing so, i.e., the path the agent visited is exactly the spiral NFC antenna. Fig. 5(d) shows an example where the red solid line marks the path the agent visited. It can be seen that the path strings many black and gray cells, and the gray cells that the agent does not visit are printed in white.

3.5 Finding the Policy by Deep Q Network

Each cell could be one of the five colors and the state space is near to $(N \times N)^5$ for an $N \times N$ sparse grid. For example, the smallest QR code (V1) is composed of 21×21 modules and its corresponding sparse grid contains $9 \times 21 \times 21$ cells, leading to nearly 10^{18} possible states. Exhaustive search is infeasible. Thus, the trick used by previous RL like Google DeepMind [29, 33] for finding $\pi(\cdot)$ is to start with a different kind of function called $Q(s, a)$, which is also known as Q-learning. The $Q(s, a)$ represents the maximum total reward that the agent can obtain by choosing action a at state s . Once $Q(s, a)$ is at hand, the policy function π can be given as follows:

$$\pi(s_k) = \operatorname{argmax}_{a_k \in \mathcal{A}} Q(s_k, a_k) \quad (6)$$

The equation is intended to choose an action for maximal $Q(s_k, a_k)$. Consequently, the function $Q(s, a)$ is a recursive formula and can be approximated using the *Bellman’s Equation*:

$$\begin{aligned} Q(s_k, a_k) &= R(s_k, a_k) + \gamma \max_{a_{k+1} \in \mathcal{A}} Q(s_{k+1}, a_{k+1}) \\ &= r_k + \max_{\mathcal{A}} (\gamma r_{k+1} + \gamma^2 r_{k+2} + \gamma^3 r_{k+3} + \dots) \end{aligned} \quad (7)$$

which is the maximal sum of reward r_k discounted by γ at each step k . The γ is a user-defined parameter that determines the agent’s horizon [29]. This equation shows that the value of $Q(s_k, a_k)$ is equal to the immediate reward r_k plus the discounted maximal value of $Q(s_{k+1}, a_{k+1})$.

DQN. We set up a five-layer fully connected neural network to parameterize an approximate $Q(s, a)$ as shown in Fig. 11. We use three hidden layers, each with a size equal to the sparse grid size. The input layer accepts the state matrix as input. The five colors will be quantified by using their gray-scale values. The output layer size is the same as the number of actions (4 in our case) since its purpose is to output the estimated Q value for each action. The LeakyReLU and MSE (Mean square error) are employed as our activation function and loss function, respectively. This neural network is called Deep Q-learning Network (DQN). Given an input

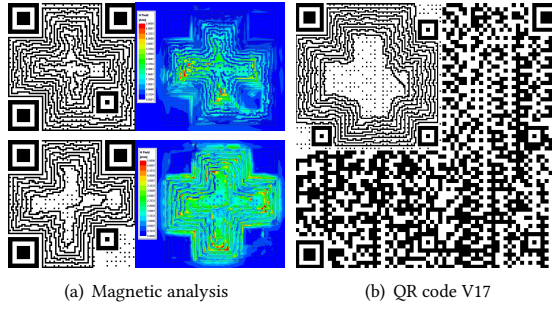


Fig. 13: Practical Discussions. (a) shows the distributions of the magnetic field when the area of alignment pattern is unblocked or blocked; (b) shows the CoilCode for a higher version QR code.

state s , DQN can estimate the Q-values for four actions. The policy $\pi(s)$ is to choose the action that results in the highest Q value. The main objective of DQN is to develop a policy $\pi(s)$ for navigating the agent successfully.

Training. The DQN is a feed-forward neural network that takes an environment state as input and yields a Q value per action. We generate the training samples by simulating thousands of random QR codes. Presumably, after playing hundreds of “games”, the agent should attain a clear deterministic policy for how to act in every possible situation and how to win the game. Correspondingly, the task is done and CoilCode is achieved once the agent wins the game. In the beginning, we simply choose a completely random policy. Then, we use it to play thousands of games through which the DQN learns and perfects how to play it. The policy $\pi(s)$ will yield considerable errors and cause the agent to lose many games at the early training states, but our rewarding policy should provide feedback on how to improve itself.

Two types of moves are used to enhance the Q-learning process: (1) *Exploitation*. These moves are dictated by the policy $\pi(s)$ as suggested by the DQN. The policy function is used in about ϵ percent of the moves before it is completed where ϵ is user-defined percent (e.g., $\epsilon = 90\%$). (2) *Exploration*. In the remaining $1 - \epsilon$ percent of moves, we take a completely random action to acquire new experiences (possibly obtain higher rewards), which the policy $\pi(s)$ may not advise because of its restrictive nature. The size of the DQN is highly related to the grid size, which is determined further by the QR version. Thus, we need to build a DQN and train it for each QR version. The training can be done on the server-side for once. We present the evolution over time in Fig. 12 regarding QR code V1, V2, and V3. For visualization purpose, we normalize the total reward between 0 and 1. It can be seen that the training well converges after about 5000 training epochs. A higher version requires much more epochs for the convergence because it contains more cells in the corresponding sparse grid.

3.6 Discussions

Three practical points are worth-noting: (1) **Cross-shaped antenna.** To validate the effectiveness of the NFC antenna designed by DQN, we use HFSS [6] to conduct magnetic field analysis using the finite element method (FEM). The top of Fig. 13(a) shows the CoilCode and the distribution of its magnetic field. We observe that the magnetic field distributes rather unevenly. After a few tests, we find that the alignment pattern on the bottom-right corner behaves as a close-loop conductive coil wrapped by the outside three turns.

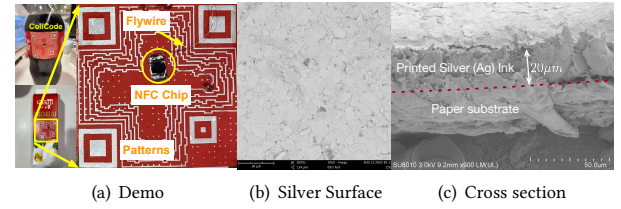


Fig. 14: Prototypes. (a) shows CoilCodes attached on objects and the zoom-in code; (b) and (c) show the surface and the cross section of CoilCode captured by SEM.

This new coil creates a new magnetic field but toward the opposite direction, which severely weakens the original field. Hence, to eliminate the negative effect of the alignment pattern, we mark the whole bottom-right corner covering the alignment pattern as a “wall” to make our coil antenna bypass this area. The bottom of Fig. 13(a) shows the new design and distribution of its magnetic field. Consequently, the average of the magnetic intensity is raised to above 2 A/m. Thus, we advise employing such a cross-shaped NFC antenna in practice. (2) **Compatibility to high version.** The QR standard (Table E.1 [24]) specifies that the version above seven contains more than one alignment pattern versions, which would raise a concern: *how do we avoid the multiple alignment patterns to support the higher version of the QR code?* The higher version QR codes are printed on a larger area. The first alignment area is sufficient to embed the coil antenna. Fig. 13(b) shows a CoilCode for a V17 QR code, in which the other alignment areas do not even require the sparsification. An NFC chip can provide more than 1 K bytes storage and thus, a single NFC antenna is enough to store the information that QR code represents.

4 IMPLEMENTATION

The main types of conductive inks on the market are metal nanoparticles, carbon nanotubes, and graphene. To date, the most conductive inks for printed electronics are based on dispersed metal nanoparticles, among which the nanosilver inks are most commonly used because they can achieve high conductivity comparable with that of bulk metal [30]. Their relative inertness also allows heat treatment under standard atmospheric conditions. After testing all three types of inks, we found that the average resistance of nanosilver-made CoilCode is around $20\ \Omega$, while resistance of CoilCode made of the carbon nanotubes and the graphene are up to $10\ k\Omega$ and $300\ \Omega$, respectively. This finding might be limited to our current craft techniques. Thus, we finally choose nanosilver inks to fabricate our prototypes. The nanosilver ink is mainly composed of Ag nanosheets (58%) and thermoplastic resin, with a viscosity of 12000-15000 cps. The conventional paper was used as the substrate for printing, and screen-printing was performed using a manual laboratory screen printer. The screen-mask mesh count is 200, 74 μm mesh opening. The blade of the squeegee is sharp, and the hardness of the scraper is 75°. Usually, the screen mask is separated from the substrate by about 2 mm. After printing is completed, the fabric is transferred to an oven at 80°C for 10 min.

The drawback of nanosilver inks is that the ink color is partial to white. As a result, it is difficult for QR code scanners to distinguish the white/black modules. To address this issue, we printed the codes on a dark-colored substrate (black or red), as demonstrated in Fig. 2(b)- Fig. 2(e). The majority of today’s QR scanners

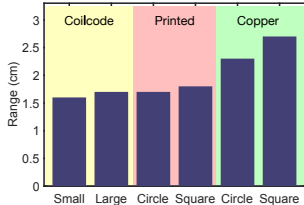


Fig. 15: Communication Range

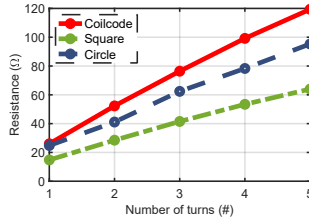


Fig. 16: Conductivity

can recognize ‘black/white’ modules through their color contrast instead of the absolute black or white. So, as long as two different colors (with distinguishable gray-values) are assigned to bit-one modules and bit-zero modules respectively, they can be successfully decoded. Fig. 14 shows the scene where CoilCode are attached to objects and the internal structure images captured by SEM (scanning electron microscope) from two views. Totally, we fabricate 200 CoilCodes with different sizes where the side length of CoilCodes varies from 5 cm to 20 cm.

5 EVALUATION

This section evaluates the performance of CoilCode in terms of NFC and barcode functionalities.

5.1 Evaluating NFC Functionality

We first evaluate the NFC functionality of CoilCodes regarding the performance of embedded coils. Before the tests, we firstly measure the physical dimensions of coils for 5×5 cm and 10×10 cm CoilCodes. Since the shape of a coil depends on the module distributions of the host QR code, the coil length varies in 85 ± 5 cm and in 170 ± 10 cm for the two sized codes, respectively. Irrelevant to QR code, the widths of the two sized codes are 0.5 mm and 1 mm respectively and the thickness of all-sized codes is maintained at $20\mu\text{m}$. Unless noted, $5 \times 5 \text{ cm}^2$ CoilCodes (the smallest size) and four turns are used by default. Subsequently, we firstly present the results of identifiability and range, and then analyze the electronic characteristics of the implanted coils.

5.1.1 Identifiability. We most care about whether the CoilCodes fabricated by conductive inks can be read successfully by the popular NFC readers with various settings. To this end, we connect four $5 \times 5 \text{ cm}^2$ CoilCodes to four mainstream COTS NFC chips: NXP NTAG 213 [11], NXP NTAG 215 [12], NXP iCODE2 [9] and FM NXP FM11RF08 [4]. Their input capacity in the matching circuits is 50, 50, 23.5, and 50 pF. Meanwhile, we employ eight types of mobile phones equipped with NFC reader modules to read the four codes. In this way, we totally have 32 different hardware settings. The transmitting power of the NFC reader is fixed at 1 Watt. The distance between the reader and the codes are set to 1.5 cm. The CoilCode is considered as being identifiable if the ID stored in

Table 2: NFC Identifiability of CoilCodes

Phone (NFC Model)	NTAG213	NTAG215	iCODE2	FM11RF08
iPhone 7 (PN67V04)	100%	100%	100%	100%
iPhone 8P (PN80V)	100%	100%	100%	100%
iPhone XR (100VB27)	100%	100%	100%	100%
iPhone 11 (SN200)	100%	100%	100%	100%
Xiaomi 9 (SN100T)	100%	100%	100%	100%
Huawei P20 (PN548)	100%	100%	100%	100%
Samsung S9 (PN80T)	100%	100%	100%	100%
Oneplus 7T (Q304)	100%	100%	100%	100%

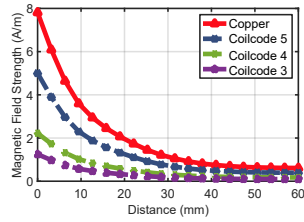


Fig. 17: Magnetic Strength

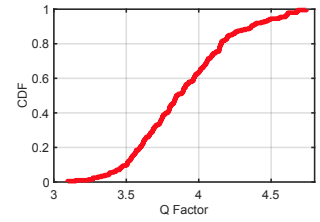


Fig. 18: Q Factor

the corresponding NFC chip is acquired successfully. We manually perform 10 trials for each setting and report the success rate. The table summarizes the reading results. In short, CoilCodes can be identified surely in all 32 settings. We also find the consistent results in other different QR codes and different sizes. Although the size and content of the host QR code affect the length of the implanted coil, the difference in the coil length is far less than the 22 m wavelength of 13.56 MHz NFC signal and thereby does not cause an evident difference when activating NFC chips. This experiment fully demonstrates that CoilCode is a general-purpose NFC solution across diverse NFC readers and chips. We also evaluate the latency of NFC identification. As a result, either identifying a coil antenna based NFC tag or identifying a CoilCode is basically instant without notable delays.

5.1.2 Communication Range. Next, we evaluate the communication range of our CoilCodes. In this experiment, we connect the two sized CoilCodes (5×5 and $10 \times 10 \text{ cm}^2$) to NTAG 213 chips. For comparison, we also measure the ranges of four other types of antenna designs: printed square coil ($5 \times 5 \text{ cm}^2$), printed circle coil ($\varnothing 5 \text{ cm}$), copper square coil ($5 \times 5 \text{ cm}^2$) and copper circle coil ($\varnothing 5 \text{ cm}$). All these coils are connected to the same model of the NFC chips and scanned by an Android phone (OnePlus 7T). In the experiment, we gradually move the reader away from a CoilCode, and the farthest recognizable distance is marked as the communication range. Fig. 15 shows the range results. We observe that (1) the ranges of copper-made coils (approximately 2.5 cm) are larger than those of the printed coils because they provide better conductivity (discussed later). (2) Even if the size is increased to $10 \times 10 \text{ cm}^2$, the range of CoilCode is still limited to 2 cm. In summary, the range of printed coils is less than that of copper coils. This is because the match circuits of current NFC chips on the market are optimized for the copper coils. However, NFC aims to identify near-field tags and thus the upper-layer applications are usually not sensitive to the communication range. On the contrary, some security or privacy-preserved applications demand a shorter range. If needed, the range can be raised essentially through increasing the thickness of the coil (i.e., printing the coils multiple times) [30].

5.1.3 Conductivity. Conductivity is a fundamental property of an antenna that quantifies how strongly it conducts electric current. To this end, we measure the resistance (in the unit of ohm) of the implanted cross-shaped coils. For comparison, we also print two standard square and circle coils using the same conductive inks. All these three types of coils are printed in an area of $5 \times 5 \text{ cm}^2$. Fig. 16 plots their resistances in a function of the number of turns. From the figure, we note the following findings: (1) resistance increases

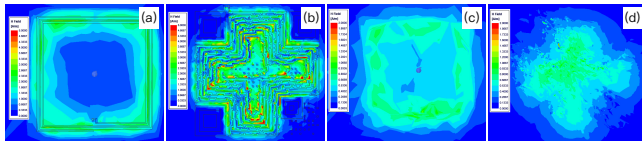


Fig. 19: Comparison of Magnetic Field. (a) and (b) show the magnetic intensity distribution of traditional square coil and CoilCode at the horizontal plane; (c) and (d) show that at the 1cm plane.

linearly from $20\ \Omega$ to around $100\ \Omega$ as the number of coil turns increases from 1 to 5. The transformer theory suggests that more coil turns can harvest more magnetic power. Thus, a trade-off in choosing the appropriate number of turns for CoilCodes exists. Our empirical studies suggest that the optimal number is 4 or 5. (2) Regardless of the shapes, the resistance of printed coil is far beyond the value of a traditional copper coil (i.e., approximately $10\ \Omega$ [10]). This relatively higher resistance results from the nature that an inkjet printed coil ($20\ \mu\text{s}$ -thick) is $25\times$ thinner than a copper antenna (0.5 mm cross-section diameter). However, this result does not affect the NFC function seriously because high resistance can be compensated by the matching circuits integrated inside today's NFC chips. (3) The resistance of a CoilCode is also higher than the two other standard coils. This phenomenon is much evident in the cases with more turns. For example, the resistance of five turns of circle coil is $64\ \Omega$, whereas that of a CoilCode is $119\ \Omega$. The reason is that the circle coil is smoothest and benefits the electron flow. By contrast, the cross-shaped coil in a CoilCode contains 13 sharp right-angles in each turn, which hinders the flow of electrons.

5.1.4 Radiation Characterization. Finally, we test the efficiency of the inductive coupling of CoilCodes. Here, our coil antennas aim to absorb energy from the magnetic field generated by the NFC reader's antenna. Interestingly, in the field of NFC, the absorption ability of an NFC chip's antenna is reflected from how strong the magnetic field it can radiate to the air due to the symmetry. Following this practice, we connect the coil antennas to a 1 Watt signal generator that produces a $13.56\ \text{MHz}$ sinusoidal signal.

(1) Magnetic Strength. The strength is measured by a Gauss Meter [5]. Fig. 17 shows the magnetic strength generated by a $5 \times 5\ \text{cm}^2$ coil antenna as functions of the distance and the number of turns (3, 4 and 5 turns). For comparison, we also measure the strength of a standard copper coil with a size of $5 \times 5\ \text{cm}^2$. Strength decreases exponentially as the meter moves away from the coils, which is in accordance with the Biot Savart Law [2]. Magnetic strength also increases when more turns are adopted. Magnetic strength approaches that of the copper-made coil. Notably, the distance here is different from the communication range, which depends not only on the NFC chip's antenna but also on the NFC reader's antenna. This experiment shows that the design of the coil antenna is reasonable in terms of the magnetic distribution.

(2) Radiation efficiency. The radiation efficiency of an antenna is evaluated using quality factor (Q factor), which measures how many times the current passes through the circuit. If an antenna has a Q factor of 4, then the current passes through its coils and capacitors four times before the energy is radiated. Higher Q factor means less circuit loss but narrower bandwidth. Generally, the recommended Q factor of commercial NFC antenna is approximately 7 [10]. We measure the Q factor of 100 CoilCodes' antennas with different QR codes and plot the CDF of the Q factor in Fig. 18. The

median Q factor of CoilCodes is 3.7, which is slightly less than the recommended value but totally acceptable in practice. The benefit of the lower Q factor provides a wider response bandwidth, making CoilCodes available in a wide range of NFC readers.

(3) Magnetic Intensity Pattern. We lastly compare the magnetic field patterns of a CoilCode's cross-shaped coil and a traditional square coil to examine the potential energy loss. The two coils are in the same size ($10\text{cm} \times 10\text{cm}$). Both are stimulated by HFSS with a 1 voltage excitation. The results are shown in Fig. 19. The magnetic field strength of both coils are very similarly, with a maximum value of $5\ \text{A/m}$ in at the horizontal plane and $2\ \text{A/m}$ at the 1cm plane. However, the two fields show a little bit different in shape. The radiation field of the square coil concentrates around the square, forming a square hollow ring; the CoilCode's field is around the center of cross and slightly shifted to the top left corner. This is mainly because the coil of CoilCode is asymmetrically recessed inward and more concentrated towards the center.

5.2 Evaluating Barcode Functionality

On the other hand, we evaluate the performance of decoding QR code in different input parameters. We adopt two main assessment criteria: bit error probability (BEP) and success rate (SR). The BEP is defined as the percent of wrongly decoded bits. It is worth noting that the BEP will be set to 100% if the QR code cannot be recognized successfully. The success rate refers to the percent of successfully decoded QR codes. Clearly, the two criteria reflect the performance on two different levels. A higher BEP does not mean a lower success rate because QR codes themselves have a relatively stronger recovery ability. By default, we use the V3 QR codes and set their error correction levels to L [24]. The decoding library, ZXing V3.4.0 [16], is used as the default decoder. We use an iPhone 11 equipped with 12-megapixel camera to scan the CoilCodes manually. The camera is fixed at a distance of 0.5 m away from the code. In addition, we also print the raw QR codes without coils and use them as baselines for performance comparison.

5.2.1 Recognizability. We first evaluate the success rate in recognizing CoilCodes with different configurations.

(1) System configurations. We test the SR across iPhone 11 (iOS), Oneplus 7T (Android) and Huawei P30 (Android). In the iOS environment, we test 3 QR code scanner apps (e.g., iOS built-in scanner, Line and WeChat). In the Android environment, we test 5 scanner apps (e.g., QR Scanner, NeoReader, SuperB Scanner Pro, QRCode Reader and QR-droid). Thus, we totally have 13 different system configurations. We use these different hardware and software settings to scan 100 randomly generated CoilCodes. Consequently, the success rates are above 99% in all cases. The only exception is the built-in barcode scanner installed in early-version Android phones, which use the absolute black/white to recognize the modules instead of the color contrast. We can print additional black coating over the nanosilver trace to resolve this backward compatibility issue. Most mainstream smart phones are all equipped with very high-resolution cameras.

(2) Resolutions. We then evaluate the SR regarding different image resolutions. To this end, we firstly use a high-resolution camera to capture the images of a CoilCode and a QR code respectively, both of which are composed of 2160×1440 pixels. Then two images

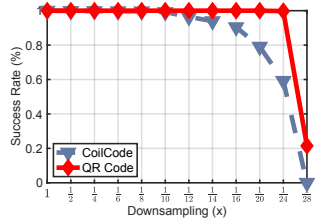


Fig. 20: SR v.s. Resolution

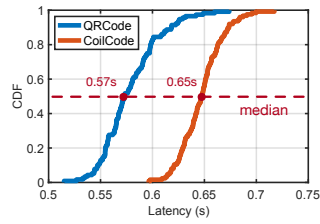


Fig. 21: Latency

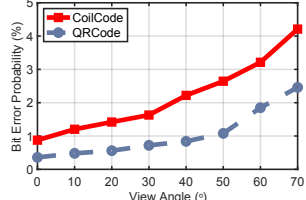


Fig. 24: BEP v.s. Angle

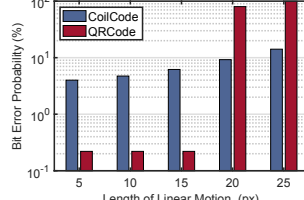


Fig. 25: BEP v.s. Blur

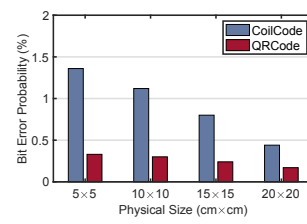


Fig. 22: BEP v.s. Size

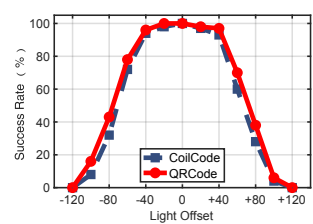


Fig. 23: SR v.s. Light

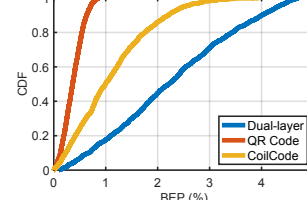


Fig. 26: BEP v.s. Flatness

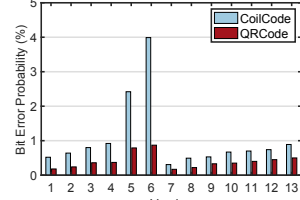


Fig. 27: BEP v.s. Version

are downsampled by a rate ranging from 1/2 to 1/28. Fig. 20 shows the SR as a function of the resolution. The SR remains unchanged when the downsampling rate is $\leq 1/10$ (or resolution $\geq 216 \times 144$). When the downsampling rate is $\geq 1/12$ (or resolution $\leq 80 \times 120$ pixels), the SR of CoilCode becomes worse than QR code. This is because the CoilCode uses the sparse QR code which removes the redundant submodules. The further downsampling might ruin the reaming center submodules. However, we would argue that such low-resolution cameras are rarely equipped for smart devices nowadays, so CoilCodes can work in absolute majority of cases.

(3) Latency. We also examine the latency when decoding QR codes and CoilCodes. As shown in Fig. 21, the medians of CoilCode and QR Code are 0.57 s and 0.65 s respectively. CoilCode takes 10% longer consumption than decoding a traditional QR codes. This is mainly because the presence of coil antenna inside a QR code might cause slight interference to the recognition in some extent, which requires more time to process. However, such small latency will be not clearly noticed by users.

5.2.2 Impact of Physical Size. The physical size of CoilCodes has a direct bearing on the decoding. In this experiment, we evaluate four sizes of CoilCodes: 5×5 , 10×10 , 15×15 and 20×20 cm 2 . The BEP results are shown in Fig. 22. BEP decreases linearly as the size increases. The BEP of the smallest CoilCode is lower than 1.4%. Regarding the lowest 7% correction level, the success rate in the four sizes are maintained at 100%. Similar results are observed for the printed raw QR codes, but their whole BEPs are approximately 0.8% lower than that of CoilCodes. This experiment shows that the presence of the implanted coil indeed affects the decoding of the QR code, but their impacts are quite limited.

5.2.3 Impact of Ambient Conditions. We adopt the common approach to testing the decoding performance of QR codes. Specifically, we first take a photo of a real CoilCode or a raw QR code, and then simulate the different ambient conditions through algorithm-based methods.

(1) Lightness. We first simulate images captured under different lightings by adding an intensity offset (-120, -100, -80, -60, -40, 0,

+40, +60, +80, +100, +120) to all pixels of the code photos. Note that the intensity is ranged from 0 to 255. Fig. 23 shows the success rate in these different settings. The rate is above 80% if the offset is within ± 40 , decreases rapidly beyond ± 40 , and reaches zero when the offset is beyond ± 120 . We also observe the similar trend when decoding raw QR codes. This experiment demonstrates that the lightness is a common factor for all types of barcodes.

(2) Orientation. We simulate images captured by different camera viewing orientations by rotating the code photos with an out-of-plane rotation angles ($10^\circ \sim 70^\circ$). The camera is exactly placed right above the image when the angle is equal to zero. Fig. 24 shows the BEPs of two types of codes from different viewing angles. Overall, the viewing angle is a key parameter that affects the decoding of barcodes. Particularly, the BEP of CoilCode is 1% higher than the QR code on average. This additional error is caused by the module splitting, which reduces the sampling area on a single module. When angle is too large, the camera may capture the non-center module by mistake. However, even 5% BEP is still under the smallest correction level of 7%.

(3) Blur. Blurry images might be captured when the user is moving or on a vehicle. To evaluate the performance in such situations, we simulate motion blurry images by applying a linear motion blur kernel to the original images, where the motion step is from 5 to 25 pixels. Fig. 25 shows the resulted BEP as a function of the motion step. As a result, we find that CoilCode is resilient to the large motions (> 15 pixel shaking) but likely to be affected by tiny motions. This is because the QR modules of CoilCode is 1/9 smaller than the normal QR code because of the downsampling. We advise to adopt the higher correction level (e.g., 30% H) or increase the size of CoilCode to prevent such potential performance degradation.

5.2.4 Impact of Flatness. The conventional dual-layer OTTC contains a relatively thicker copper coils in the hidden layer, making the QR code be printed on an uneven surface. We study the impact of the flatness on the BER of recognizing a dual-layer OTTC compared with a pure QR code and a CoilCode. We fabricate dual-layer codes by attaching printed QR codes onto commercial NFC coils. The codes are in the size of 5×5 cm 2 . As shown in Fig. 26, the

median BEP of dual-layer OTTC is 1.8% and 1% higher than that of the traditional QR codes and CoilCodes. This shows that flatness indeed affects the recognition of QR codes. In contrast, CoilCodes can be considered as flat as the QR code since the conductive ink is $20\mu\text{m}$ thick, which cannot be distinguished by optical cameras.

5.2.5 Impact of QR Code Version. Next, we test the impact of the version on BEP. In the experiment, we print 13 copies of CoilCodes or QR codes using different versions. Blank data will be padded to the QR code if the data size is less than the maximal capacity. The results are plotted in Fig. 27. The BEP increases as the version rises when $V < 7$. Clearly, higher version QR codes can encode more bits and become denser in a fixed area, thereby increasing the BEP. The highest BEP of 4% is observed at version 6. However, when $V \geq 7$, the physical size of the QR code must be enlarged by 4x because it itself is too dense to accommodate more bits [24]. As shown in Fig. 13(b), CoilCodes only take up the top-left corner to implant the coil antenna. As a result, the BEPs of the versions higher than 7 fall suddenly and remain at a low level (less than 1%).

6 RELATED WORK

Our design involves many fields. In this section, we introduce the most related work. **(1) Chipless RFID.** Chipless RFID tags are RFID tags that do not require microchips in the transponders. They can be identified through the different patterns of antennas (called planar encoders). They are considered a promising replacement of optical barcode with the use of low-cost conductive inks [17, 22, 32]. Unfortunately, this technique has never been used outside of a laboratory because of its vulnerability to environmental noise and other fatal weaknesses. Better than chipless RFIDs, which must be scanned by special readers, CoilCode can be identified by today's smart devices equipped with NFC. **(2) Aesthetic QR codes.** Aesthetic QR codes aim at beautifying the visually unpleasant appearance of QR codes [18, 20, 27, 28], which inspired us to generate the sparse code. For example, Peled et al. [14] developed a visual QR code generator called Visualead, which retained the original contrast between the encoding modules and the blended image to synthesize aesthetic QR codes. Chu et al. [18] presented a novel style aesthetic QR code called halftone QR codes, which subdivided each module of the standard QR code into 3×3 submodules. Lin et al. [27] synthesized an aesthetic QR code based on the Gauss Jordan elimination used in the QArt method. Zhang et al. [37] relocated the modules of the QR code that depend on visual saliency. Xu et al. [35] adopted a transfer network for stylizing the aesthetic QR codes with different styles. **(3) Printed Electronics.** Our work is also inspired by the recent development in printed electronics [21, 25, 30, 31]. For example, Mujal et al. [30] employed silver nanoparticle inks to fabricate an NFC antenna. He et al. [21] utilized the conductive graphene ink to print circuits. Hou et al. [23] also fabricated graphene passive electronic skin for human touch. Li et al. [26] created a foldable supercapacitors using reduced graphene oxide. Pan et al. [31] employed multilayer graphene ink to create wideband wireless antennas. Differing from these previous works, our focus is on designing the NFC antenna inside a QR code. Generally, CoilCode can be implemented with the newly invented conductive inks. **(4) Reinforcement Learning.** Our work is also inspired by

many previous RL work, such as AlphaGo [33], Atari [33], MOBA Game [34], and so on.

7 LIMITATIONS & FUTURE WORK

Finally, we present the current limitations and future work in this section.

Limitations. The current prototype requires a relatively complicated printing procedure due to the limitation of our fabrication hardware. The purpose of our prototype is to verify the feasibility and practicality of our idea. However, we can vision that the codes can be directly printed by user-friendly electronic printers in the near future. In addition, CoilCode still requires to connect an NFC chip to the printed coil antenna. The ideal case is to print a chipless RFID by using the conductive inks directly. However, today's NFC readers are not compatible with chipless RFIDs. We have to achieve such a trade-off solution at present.

Future Work One of the main contributions of this work is to leverage the advances of RL to design an embedded coil antenna. Such an RL framework can be also utilized to explore many other potential applications: **(1) Design of Chipless RFIDs.** The majority of the current chipless RFIDs use the response frequencies to encode the ID. Unfortunately, the limited bandwidth constraints the range of encodable IDs. We could utilize this framework to explore the spatial spectrum rather than the frequency spectrum to design new chipless RFIDs. **(2) Design of diverse antennas.** To the best of our knowledge, our effort is one of the few pioneer works that attempts to utilize the AI to design new antennas. We will continue to leverage this RL-framework to explore new and highly efficient antennas like massive MIMO antenna array. **(3) Design of OTTC-friendly barcodes.** On the other hand, we can also use the framework to design new optical barcodes, which are different from QR codes but more friendly to embedded antennas. **(4) Design of aesthetic QR codes.** Similarly, the framework can also work for designing new aesthetic QR codes. **(5) Design of new games.** Our framework might be leveraged to design such new games personalized to individual players. For example, it will be funny to play a maze game where the maze is generated from the QR code of the player's name.

8 CONCLUSION

This work presents CoilCode, which is a system that incorporates NFC tag and QR code in a single printed paper. Achieving the RF functionality of an NFC antenna and the optical properties of a QR code using conductive ink is challenging. CoilCode combines classical RF circuit theory and reinforcement learning to address this problem. We believe this work will pave the way for exciting new directions for the exploration of flexible electronic communications.

ACKNOWLEDGMENTS

This study is supported in National Key R&D Program of China 2019YFB2103000, NSFC Key Program (No. 61932017), NSFC Excellent Young Scientists Fund (Hong Kong and Macau) (No. 62022003), NSFC General Program (No. 61972331), Hong Kong General Research Fund (No. 15204820). The research of Dr. Shan Chang was supported in part by the National Natural Science Foundation of China (No. 61972081). We thank all the anonymous reviewers and the shepherd, for their valuable comments and helpful suggestions.

REFERENCES

- [1] Apple Clips. <https://developer.apple.com/app-clips/>.
- [2] Biot-savart law. https://en.wikipedia.org/wiki/Biot%20%80%93Savart_law.
- [3] Deep Reinforcement Learning for Maze Solving. <https://www.samyzaf.com/ML/r/qlmaze.html>.
- [4] FM11RF08. <https://www.sport-consulting.net/wp-content/uploads/2017/03/CHIP-MAIFER.pdf>.
- [5] Gauss meter. https://www.pce-instruments.com/english/measuring-instruments/test-meters/gauss-meter-tesla-meter-pce-instruments-gauss-meter-pce-mfm-3500-det_593255.htm?_list-kat&_listpos=5.
- [6] HFSS. <https://www.ansys.com/products/electronics/ansys-hfss>.
- [7] Longest Path Problem. https://en.wikipedia.org/wiki/Longest_path_problem.
- [8] Maze Game. <https://en.wikipedia.org/wiki/Maze>.
- [9] NXP ICODE. https://www.nxp.com/products/rfid-nfc/nfc-hf/icode:MC_42024.
- [10] Nxp nfc antenna design guide. <https://www.nxp.com/docs/en/application-note/AN11740.pdf>.
- [11] NXP NTAG 213. https://www.nxp.com/products/rfid-nfc/nfc-hf/icode:MC_42024.
- [12] NXP NTAG 215. https://www.nxp.com/products/rfid-nfc/nfc-hf/icode:MC_42024.
- [13] Snake Game. [https://en.wikipedia.org/wiki/Snake_\(video_game_genre\)](https://en.wikipedia.org/wiki/Snake_(video_game_genre)).
- [14] Visualead. <https://www.visualead.com/>.
- [15] Zebra RFID Printers. <https://www.zebra.com/ap/en/products/rfid/rfid-printers.html>.
- [16] ZXing 3.4.0. <https://github.com/zxing/zxing/releases/tag/zxing-3.4.0>.
- [17] BALBIN, I., AND KARMAKAR, N. C. Phase-encoded chipless rfid transponder for large-scale low-cost applications. *IEEE microwave and wireless components letters* 19, 8 (2009), 509–511.
- [18] CHU, H.-K., CHANG, C.-S., LEE, R.-R., AND MITRA, N. J. Halftone qr codes. *ACM Transactions on Graphics (TOG)* 32, 6 (2013), 1–8.
- [19] FRANÇOIS-LAVET, V., HENDERSON, P., ISLAM, R., BELLEMARE, M. G., AND PINEAU, J. An introduction to deep reinforcement learning. *arXiv preprint arXiv:1811.12560* (2018).
- [20] GARATEGUY, G. J., ARCE, G. R., LAU, D. L., AND VILLARREAL, O. P. Qr images: optimized image embedding in qr codes. *IEEE transactions on image processing* 23, 7 (2014), 2842–2853.
- [21] HE, P., CAO, J., DING, H., LIU, C., NEILSON, J., LI, Z., KINLOCH, I. A., AND DERBY, B. Screen-printing of a highly conductive graphene ink for flexible printed electronics. *ACS applied materials & interfaces* 11, 35 (2019), 32225–32234.
- [22] HERROJO, C., PAREDES, F., MATA-CONTRERAS, J., AND MARTÍN, F. Chipless-rfid: a review and recent developments. *Sensors* 19, 15 (2019), 3385.
- [23] HOU, C., WANG, H., ZHANG, Q., LI, Y., AND ZHU, M. Highly conductive, flexible, and compressible all-graphene passive electronic skin for sensing human touch. *Advanced Materials* 26, 29 (2014), 5018–5024.
- [24] ISO, I. 18004: 2006 (2006) information technology—automatic identification and data capture techniques—qr code 2005 bar code symbology specification. *International Organization for Standardization, Geneva, Switzerland*.
- [25] KAMYSHNY, A., AND MAGDASSI, S. Conductive nanomaterials for printed electronics. *Small* 10, 17 (2014), 3515–3535.
- [26] LI, J., SHAO, Y., SHI, Q., HOU, C., ZHANG, Q., LI, Y., KANER, R. B., AND WANG, H. Calligraphy-inspired brush written foldable supercapacitors. *Nano energy* 38 (2017), 428–437.
- [27] LIN, S.-S., HU, M.-C., LEE, C.-H., AND LEE, T.-Y. Efficient qr code beautification with high quality visual content. *IEEE Transactions on Multimedia* 17, 9 (2015), 1515–1524.
- [28] LIN, Y.-H., CHANG, Y.-P., AND WU, J.-L. Appearance-based qr code beautifier. *IEEE Transactions on Multimedia* 15, 8 (2013), 2198–2207.
- [29] MINIH, V., KAVUKCUOGLU, K., SILVER, D., RUSU, A. A., VENESS, J., BELLEMARE, M. G., GRAVES, A., RIEDMILLER, M., FIDJELAND, A. K., OSTROVSKI, G., ET AL. Human-level control through deep reinforcement learning. *nature* 518, 7540 (2015), 529–533.
- [30] MUJAL, J., RAMON, E., DÍAZ, E., CARRABINA, J., CALLEJA, Á., MARTÍNEZ, R., AND TERÉS, L. Inkjet printed antennas for nfc systems. In *Proc. of IEEE ICECS* (2010).
- [31] PAN, K., FAN, Y., LENG, T., LI, J., XIN, Z., ZHANG, J., HAO, L., GALLOP, J., NOVOSELOV, K. S., AND HU, Z. Sustainable production of highly conductive multilayer graphene ink for wireless connectivity and iot applications. *Nature communications* 9, 1 (2018), 1–10.
- [32] PRERADOVIC, S., AND KARMAKAR, N. C. Chipless rfid: Bar code of the future. *IEEE microwave magazine* 11, 7 (2010), 87–97.
- [33] SILVER, D., HUANG, A., MADDISON, C. J., GUEZ, A., SIFRE, L., VAN DEN DRIESSCHE, G., SCHRITTWIESER, J., ANTONOGLOU, I., PANNEERSHELVAM, V., LANCTOT, M., ET AL. Mastering the game of go with deep neural networks and tree search. *nature* 529, 7587 (2016), 484–489.
- [34] WU, B. Hierarchical macro strategy model for moba game ai. In *Proc. of AAAI* (2019).
- [35] XU, M., SU, H., LI, Y., LI, X., LIAO, J., NIU, J., LV, P., AND ZHOU, B. Stylized aesthetic qr code. *IEEE Transactions on Multimedia* 21, 8 (2019), 1960–1970.
- [36] YANG, L., CHEN, Y., LI, X.-Y., XIAO, C., LI, M., AND LIU, Y. Tagoram: Real-time tracking of mobile rfid tags to high precision using cots devices. In *Proc. of ACM MobiCom* (2014).
- [37] ZHANG, Y., DENG, S., LIU, Z., AND WANG, Y. Aesthetic qr codes based on two-stage image blending. In *Multimedia Modeling* (2015), Springer, pp. 183–194.